Supporting Information for:

"K$^+$, Na$^+$, and Mg^{2+} on DNA Translocation in Silicon Nitride Nanopores"

by James Uplinger, Brian Thomas, Ryan Rollings, Daniel Fologea, David McNabb, Jiali Li

SI.1 the time responses of the Axopatch system and the nanopore membrane

The time measurements are a crucial aspect of this manuscript. To ensure the times are measured accurately, we calibrated the time responses of both the Axopatch and a nanopore membrane sample. With the Axopatch Low-Pass Bessel-Filter set at above 10 kHz (Fig. S1), the section **SI.1a** next shows that the time durations could be measured accurately up to 25 μs. The section **SI.1b** shows the time responses of a nanopore membrane sample is less than 20 μs (Fig. S2).

SI.1a. Calibration the time response of the Axopatch at 10 kHz low pass filter

Ionic current through solid state nanopores was measured and recorded using an integrated Axopatch 200B patch-clamp amplifier system (Molecular devices) in resistive feedback mode. The 10 kHz Low Pass Bessel (LPB) filter in the Axopatch 200B was selected for some measurements in this work. The filter is implemented as an analog circuit; therefore, to determine its influence on the time measurements we performed a series of control experiments. The whole measurement system was tested and calibrated with artificial current drops generated by ideal square pulses from a function generator (Agilent 33250A). The calibration signal and analysis appears in Figure S1.
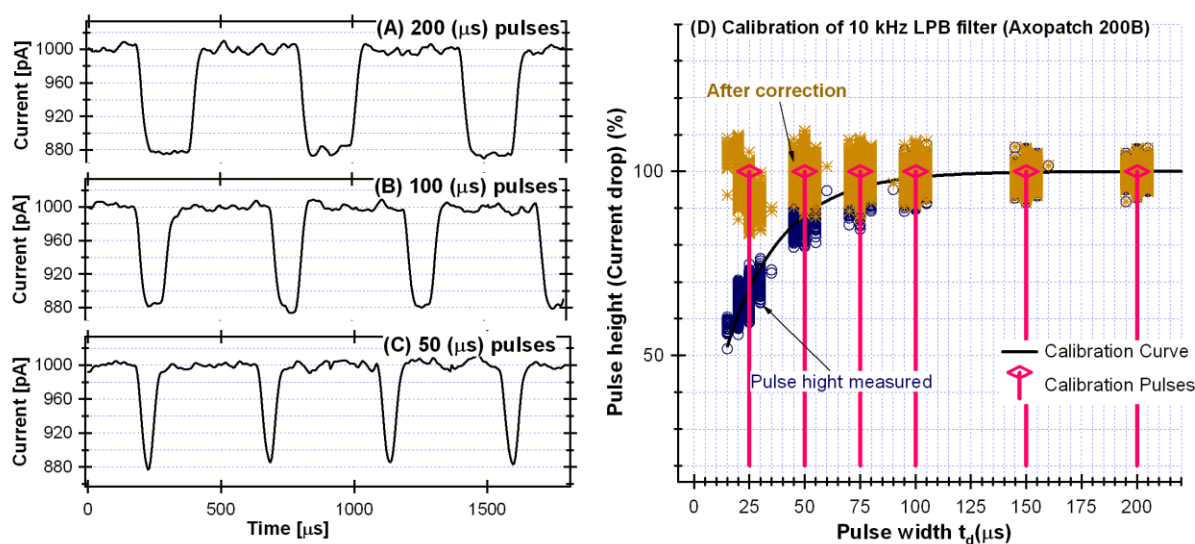

Fig. S1: Calibration of the 10kHz Low-Pass Bessel-Filter (Axopatch 200B) Response with ideal square current drops.

The ideal pulse widths generated were 25, 50, 75, 100, 150, 200, and 300 μsec. The pulse height was about 100 pA with a rise time of 5 ps. Examples of the 10 kHz filter responses to these pulses recorded are shown in Fig. S1. (A) for 200 μs, (B) for 100 μs, and (C) for 50 μs pulses. The recorded artificial current drop events were analyzed with the same MatLab routines used for analyzing real DNA current drop signal. The measured mean pulse heights ΔI_b verses the pulse widths t_d are plotted in Fig. S1(D) (blue circles).

This calibration shows that when the pulse width is less than 100 μsec, the calculated mean pulse height will be attenuated, but the time durations (the width of half height) remain correct up to 25 μsec pulses. When the time duration measured in our work was less than 100 μs, the current blockage amplitude can be corrected (S1D, tan stars) with this calibration as shown.

SI.1b. The time response of a nanopore sample at 10 and 100kHz

Keeping all other conditions the same, below we show how the 10 and 100 kHz filter affects the amplitude ΔI_b and time duration t_d of current blockage events measured with a DNA sample in a nanopore. The data presented here were taken with a 10 nm pore in 1.6 M KCl with 20% glycerol and TE buffer solution at pH 8. A linearized 3 kbp DNA pSP65 was used for the experiment. The current blockage events were recorded with the LPB filter set at 100, 50, 10, 5, 2 and 1 kHz. The applied voltage was 200 mV.

The event distribution plots show that the current blockage amplitude is slightly smaller for ΔI_b measured with LPB filter set at 10 kHz (Fig. S2 (A), the most probable ΔI_b is 310 pA) compared to the LPB filter set at 100 kHz (Fig. S2 (B), the most probable ΔI_b is 300 pA). Examples of the current blockage events measured with LPB filter set at 10 kHz filter (insert in Fig. S2 (B)) and at 100 kHz filter (insert in Fig. S2 (A)) further show the difference in detail for the events measured at these two LPB filter settings at which all the data were recorded in this paper.

To compare the time responses at different filter settings, we analyzed the fall and rise times of the DNA translocation events as a function of the filter frequency (Fig. S2 (C)). The analysis in Figure S2 (C) shows that the Fall and Rise times are ~20 μs with LPB filter set at 100 kHz and ~25 μs at 10 kHz, well below the t_ds measured in this paper ($t_d \geq 50$ μs, Fig. 3A). However, if the LPB filter was set at above 5 kHz, the response times increased significantly. Using the applied voltage (Ψ) and open pore current (I_0), the estimated nanopore resistance was ~40 MΩ, with a response time about 20 μs the nanopore membrane has, the estimated membrane capacitance was in the order of ~1pF for this nanopore sample.
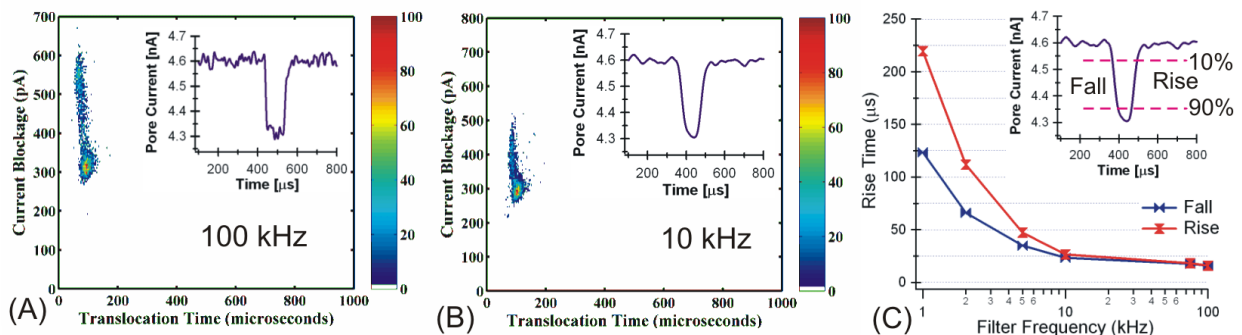
Fig. S2: The event number density plots of 100 kHz (A) and 10 kHz (B) Low-Pass Bessel-Filter for the 3 kbp DNA events. The fall and rise times of translocation events measured as a function of the filter bandwidth (C). The fall and rise time was measured between the 10% and 90% height of the events as illustrated in (C).

In summary, the above analysis shows that the time response of a nanopore membrane (**SI. 1b**) is less than ~20 μs. Therefore, the membrane capacitance would not be the limiting factor of the time durations (t_ds) measured in this work ($t_d \geq 50$ μs, Fig. 3A).

SI.2 Verification of DNA translocation through silicon nitride nanopores
-by PCR amplification and gel electrophoresis of the *trans* chamber sample

In our previously published results on DNA translocation in Ion Beam Sculpted solid-state nanopores [1-4], we have studied how the current blockage signal changes as a function of DNA length, DNA conformation (ss, ds, circular, supercoiled), applied voltage, solution viscosity, and solution conductivity (salt concentration). All our observations have supported or have been consistent with the conclusion that the DNA molecules had traversed through the nanopores. However, the length of the DNA molecules used in our previous nanopore experiments were 2.7 kbp or longer, and, we had not demonstrated directly that the DNA molecules were translocated through the Ion Beam Sculpted solid state nanopores. In this experiment, we provide such a proof using a ~1000 base pair long dsDNA.

SI.2a. The DNA used. We used a 1 kbp linear double strand DNA segment that was generated by PCR amplification of a DNA fragment from PhiX174 genomic DNA (New England Biolabs). The success of the PCR reaction to obtain the 1 kbp dsDNA segment was verified by agarose gel electrophoresis **(**data not shown here**).**

SI.2b. The translocation Experiment. A ~10 nm diameter pore (measured by TEM image) was used for this experiment. The experiment was performed in our standard salt solution: 1M KCl in TE buffer at pH 7. The bias voltage was 120 mV. The average open pore current was I_0=11±1.5 nA during the entire time of the recording. We estimate the nanopore diameter is about ~10 nm based on this open pore current. No transient current drop events were observed before the DNA was added to the *cis* chamber. After the 1kbp dsDNA was added, the estimated concentration of the 1 kbp DNA was10 nM in the *cis* chamber. Approximately 40,000 current blockage events were recorded and the experiment lasted about 4 hours.

We characterize every current blockage event by its mean current blockage amplitude (ΔI_b) and its time duration (t_d) and we show our results in an event distribution plot. Figure S3 (A) shows the event number density distribution of the current blockages recorded. It shows that the most probable current drop values are at $\Delta I_b \approx 112$ pA and $t_d \approx 60$μs.

SI.2c. PCR amplification and gel electrophoresis of the trans chamber sample. Shorter DNA translocations through α-hemolysin channel[5] and solid state nanopores[6] from *cis* to *trans* chamber have been verified by gel electrophoresis. To prove that a longer ~1 kbp DNA had traversed from the *cis* to the *trans* chamber during the ~4 hours recording time while the ~40,000 current blockage events occurred, we collected samples (~50 μl each) from the *trans* chamber

before (as a control) and after the DNA was added to the *cis* side. The control and *trans* samples were amplified 30 rounds by PCR, separated using agarose gel electrophoresis, and photographed after staining with ethidium bromide to determine final DNA size. Positive and negative controls were also run using the same PCR reagents and thermal cycler to reduce the chance of false negatives or positives. Fig. S3 (B) shows the gel electrophoresis results that demonstrated the 1kb dsDNA had traversed the solid-state nanopore during the translocation experiment. We estimated that the number of DNA molecules translocation through the pore is consistent with the number of blockage events observed.

The lane 2 and lane 3 of the gel show that our PCR parameters were sufficient to amplify the DNA of interest and that we were free of contamination. The lane 4 (*trans* sample before the 1 kbp DNA was added to the *cis* side) has no 1kbp dsDNA while the lane 5 shows a clear 1kbp band. This shows that the 1 kbp DNA was present in the *trans* chamber only after DNA was added to the *cis* chamber, demonstrating that the 1 kbp DNA translocated through the nanopore from the *cis* to the *trans* chamber and further supporting the interpretation of transient current blockages as being caused by single DNA molecules translocating through the pore.
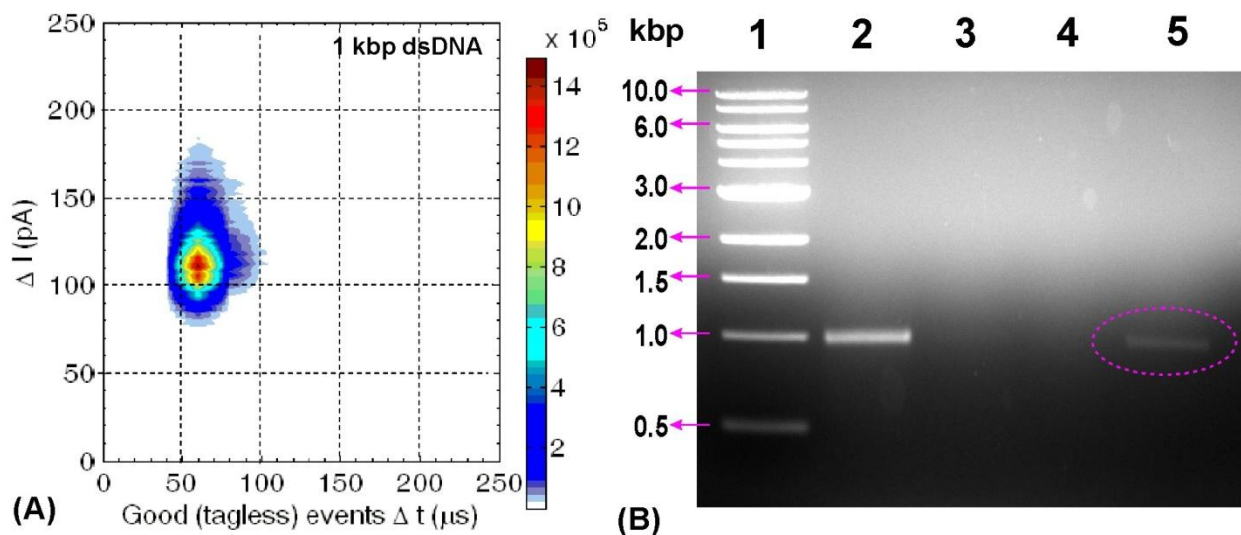

Fig. S3. (**A**) Distribution of current blockage events measured from the 1kb dsDNA molecules. The average open pore current was $I_0=11\pm1.5$ nA during the time of the recording. We estimate the nanopore diameter is about 10 nm based on this open pore current. The most probable current drop values are at 112 pA and 60μs. (**B**) Agarose gel electrophoresis to demonstrate that the 1kb dsDNA traversed the solid-state nanopore. **Lane 1**. Promega Corp. 1 kbp DNA ladder, **Lane 2**, Positive control for the *cis* chamber sample (10^8 dilution), **Lane 3**, negative control with no template DNA, **Lane 4**, trans chamber solution before the DNA was added, **Lane 5**, trans sample collected after ~40,000 events were recorded. Photograph of the ethidium bromide-stained gel was taken using UV transillumination in a FluoroChem 8900 imaging system.

SI.3 Details of current blockage events analysis

Current blockage events are characterized by their average current drop amplitude ΔI_b and their time duration t_d as illustrated in Fig 1(E). The current blockage events were recorded in event driven mode. Pre- and post-trigger length was 500 samples (Open pore current data points). The recorded data then were analyzed using custom Matlab® routines. These routines include baseline correction, events classification, and calculation of ΔI_b and t_d. For events detection and classification, the start of a current blockage event was defined as one that caused the nanopore current to drop monotonically below two thresholds; the end of the event was signaled by the current trace climbing monotonically back to the open channel current past both of these thresholds. The event duration, t_d, was defined by the time between the current drop across the second threshold. The second threshold was set to be at 50% of the most probable peak value of the current blockages. The arithmetic mean of the current blockage value (ΔI_b) was calculated within the range between the crossings of the second threshold. Current blockage events with t_d <30 μs were not selected in this work.

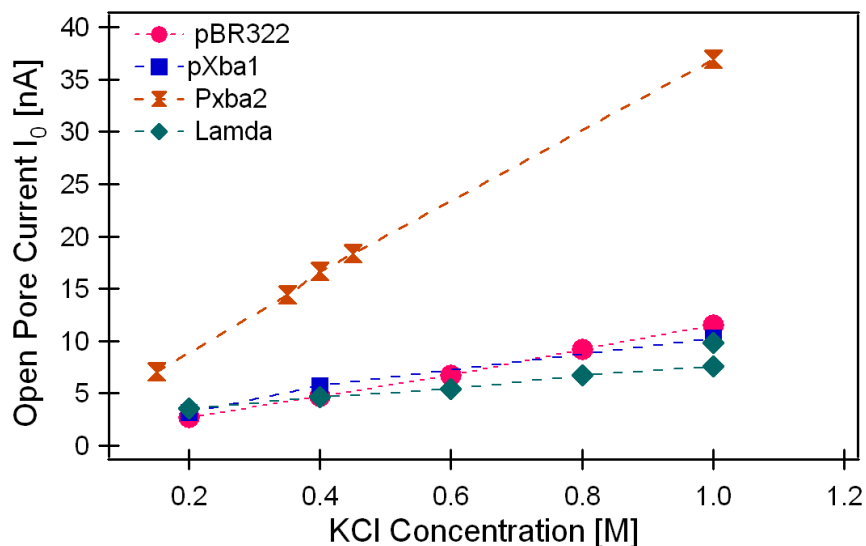## SI.4 Open pore current I_0 for data in Figure 3

Fig. S4. The open pore current $\mathbf{I_0}$ as a function of KCl concentration for the data displayed in Figure 3.

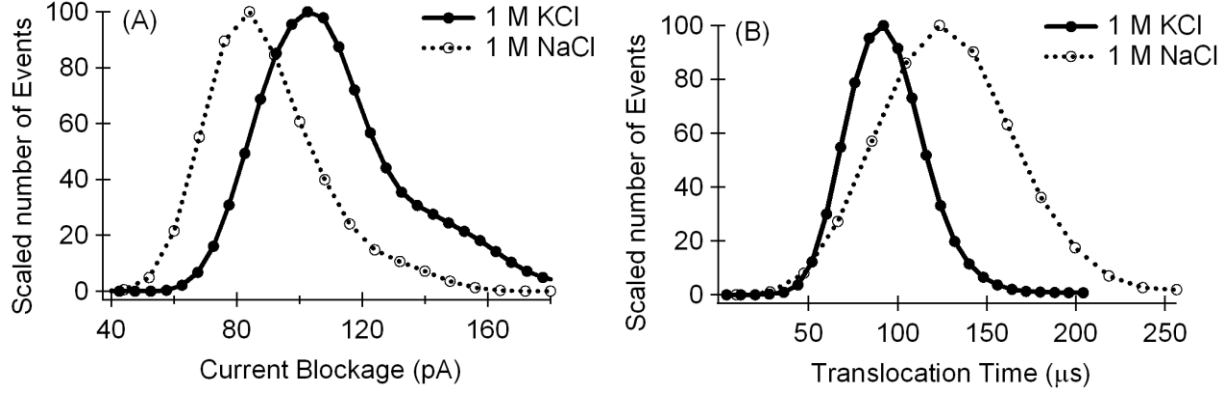## SI.5 3 kbp linear dsDNA (pSP65) in 1M NaCl versus in 1M KCl

Fig. S5. (A) Current blockage histograms for the linear 3 kbp DNA molecules in the monovalent salts NaCl and KCl. (B) Translocation duration times histograms for the DNA in NaCl and KCl solutions. A ~12 nm diameter nanopore was used for this experiment.

SI.6 Manning Counterion Condensation (MCC) theory

In Manning Counterion Condensation (MCC) theory [7], a highly charged DNA molecule tends to lower its effective charge by counterion binding. For a solution that contains monovalent or divalent ions or a mixture of both, the effective charge per phosphate, Q, of a DNA molecule is lowered from the elementary charge q by a factor of [1- $(\theta_1 + 2\theta_2)$] [7-9]:

$$Q = q(1 - \theta_1 - 2\theta_2) \tag{S1}$$

Here θ_1 and θ_2 are the number of associated bound counterions per phosphate for monovalent and divalent cations respectively. The equations for determining θ_1 and θ_2 in a solution of known concentration of monovalent ion C_1 and divalent ion C_2 are

$$\ln(1000e\theta_1 / C_1 V_{P1}) = -2\xi(1 - \theta_1 - 2\theta_2)\ln(1 - e^{-\kappa b}) \tag{S2}$$

$$\theta_2 / \theta_1^2 = 1000e(V_{P2} / V_{p1}{}^2)C_2 / C_1^2 \tag{S3}$$

Here $V_{pz} = 4\pi e N_0 (1 + Z)(\xi - Z^{-1})b^3$ is the volume around a DNA in which the counterions (Z=1 for monovalent and 2 for divalent) are considered to be territorially bound (cm^3/mole P) [8], N_0 is Avogadro's number, ξ=(q^2/εb)/k$_b$T=4.2 at 25°C is defined by the ratio of the electrostatic repulsion energy of adjacent charges on the DNA to the thermal energy, e≈2.718 is the base of nature logarithms, and κ is the Debye- screening parameter [7]. For a B type double stranded DNA in aqueous solution, the average axial charge spacing b = 3.4 Å /2e = 1.7 Å/e [7]. By solving Eq. 2 and Eq. 3 numerically, the relation of θ_1 and θ_2 as a function of C_1 and C_2 can be found, thus the effective charge Q as a function of salt solution can be estimated theoretically from using Eq. (S1). Using $t_d \sim 1/Q$, or t_d^0/t_d=Q/Q^0 where t_d^0 or Q^0 is a reference point, we can calculate the change in DNA translocation time predicted by MCC theory.

The number of bound counterions θ_1 and θ_2.

The theoretically calculated changes in Q using Eqs. S1, S2 and S3 are shown as dotted lines in Figures 7C. These data indicate a smaller change in Q at higher divalent salt concentrations as compared to the measured values, but the values are within experimental error. The values of V_{pz} calculated from the definition are V_{p1}=646 cm^3/mol P and V_{p2} =838 cm^3/mol P calculated by $V_{pz} = 4\pi e N_0 (1+Z)(\xi - Z^{-1})b^3$.

When there is no divalent ion present in the solution, θ_2=0, Eqs. S1 and S2 can predict monovalent salt concentration effect. The MCC theory calculated change in t_d is shown as the solid line in Fig. 3B.

SI.7 Event frequency as a function of KCl concentration

Table S1. The event frequency evolution as a function of KCl concentration is given in the table below.

KCl [M]	Debye length $\lambda_D = 0.303/\sqrt{c}$ [nm]	λ DNA Event Frequency [Hz]	pXba1 Event ration C/SC	pXba1 Event Fre. [Hz]	pXba2 Event Fre. [Hz]	pBR322 Event Fre. [Hz]
		$D_p \sim 10$ nm	$D_p \sim 10$ nm		$D_p \sim 25$ nm	$D_p \sim 10$ nm
0.15	0.78				10	
0.2	0.68	3.6	28%	2.0		3
0.35	0.50				10	
0.4	0.48	2.6	23%	2.4	9	15
0.45	0.45				10	
0.6	0.39	4.8				33
0.8	0.34	4.0				50
1.0	0.30	0.9	19%	3.9	56	12

Some of the recorded data traces contained events with very long t_ds and longtime intervals between events, the data in the table are only for comparisons and errors were not estimated. The Debye length (in nm) was calculated from $\lambda_D = 0.303/\sqrt{c}$, where c is the Molar concentration of KCl [10, 11].

Interestingly, the event frequency range is similar to a strong negatively charged polymer dextran measured with α-hemolysin pores[12]. These data also show that at higher salt concentrations or shorter Debye length, the event frequency tends to increase with ~10 nm pores* except for 2 points at 1M KCl. For the larger ~25 nm pore with the same pXba DNA, the event frequency was several times higher.

REFERENCES

[1] Li, J., Gershow, M., Stein, D., Brandin, E., Golovchenko, J. A., Nat. Mater. 2003, 2, 611-615.

[2] Fologea, D., Gershow, M., Ledden, B., McNabb, D. S., et al., Nano Lett. 2005, 5, 1905-1909.

[3] Fologea, D., Uplinger, J., Thomas, B., McNabb, D. S., Li, J., Nano Lett. 2005, 5, 1734 - 1737.

[4] Fologea, D., Brandin, E., Uplinger, J., Branton, D., Li, J., Electrophoresis 2007, 28, 3168-3192.

[5] Kasianowicz, J. J., Brandin, E., Branton, D., Deamer, D. W., Proc. Natl. Acad. Sci. U.S.A. 1996, 93, 13770-13773.

[6] Heng, J. B., Ho, C., Kim, T., Timp, R., et al., Biophys. J. 2004, 87, 2905-2911.

[7] Manning, G. S., Q. Rev. Biophys. 1978, 2, 179-246.

[8] Rhee, K. W., Ware, B. R., J. Chem. Phys. 1983, 78, 3349-3353.

[9] Li, A. Z., Huang, H., Re, X., Qi, L. J., Marx, K. A., Biophys. J. 1998, 74, 964-973.

[10] Ghosal, S., Phys. Rev. Lett. 2007, 98.

[11] Probstein, R., Physicochemical Hydrodynamics, Wiley, New York 1994.

[12] Oukhaled, G., Bacri, L., Mathe, J., Pelta, J., Auvray, L., Europhys Lett, 2008, 82.